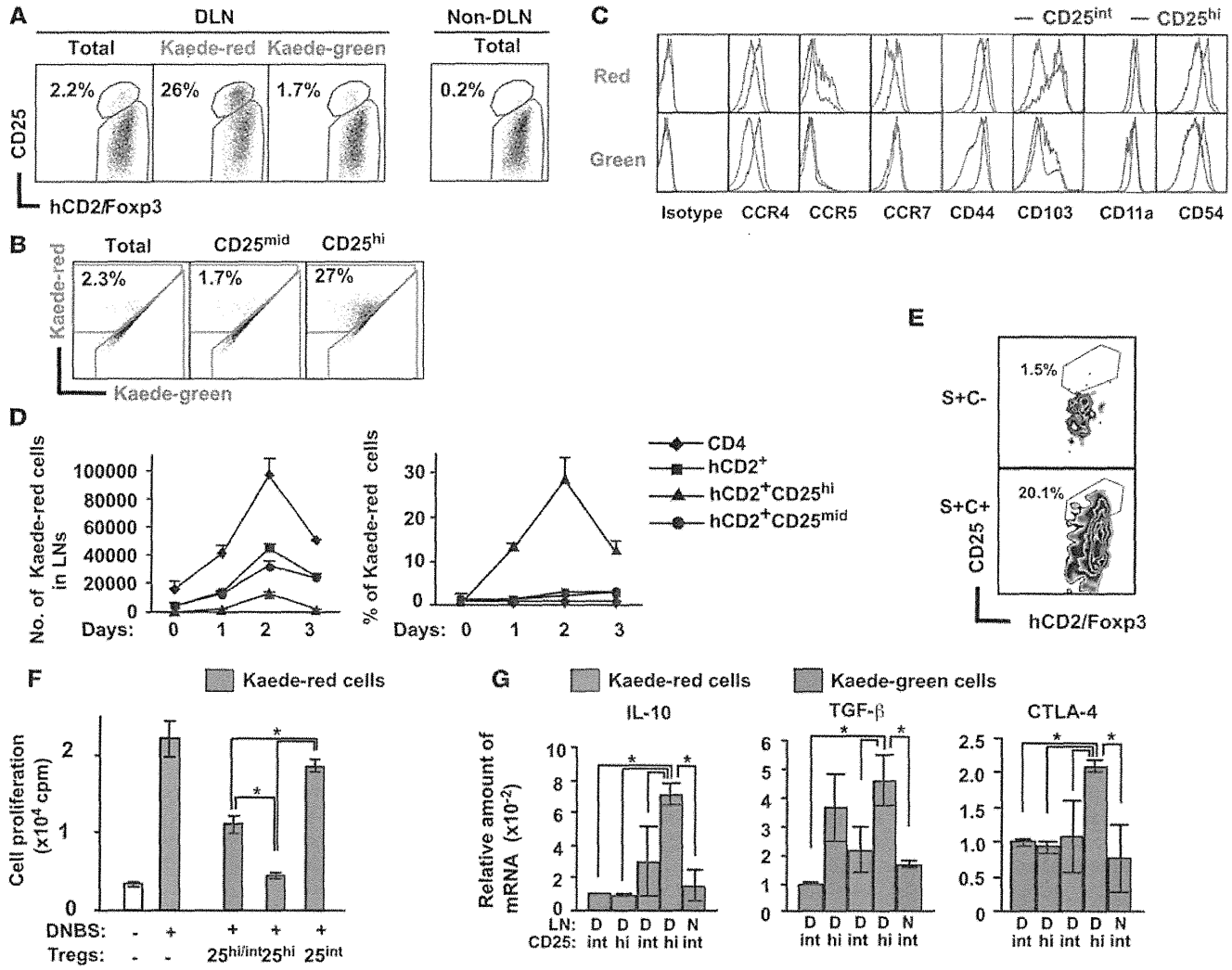

Figure 7

Kinetics and suppression activity of CD25^{hi} Kaede-red migratory Tregs. (**A–C**) Characterization of CD25^{hi} subset. Kaede/Foxp3$^{hCD2/hCD52}$ mice were treated as in Figure 3A, and the expression levels of hCD2/Foxp3 and CD25 on CD4^{+}hCD2/Foxp3^{+} Tregs in total, Kaede-red, and Kaede-green DLN cells and in non-DLN cells (**A**), the frequency of Kaede-red populations in each population (**B**), and the expression levels of surface markers on Kaede-red or Kaede-green Tregs in the DLNs (**C**) were analyzed. (**D**) Kinetics of T cell migration. Kaede/Foxp3$^{hCD2/hCD52}$ mice were sensitized and challenged as in Figure 3A and photoconverted immediately (day 0), 1 (day 1), 2 (day 2), or 3 (day 3) days after challenge. The number of each subset migrating for 24 hours after photoconversion and the frequency of Kaede-red cells among each subset were measured. (**E**) Foxp3$^{hCD2/hCD52}$ mice were sensitized with DNFB (S+) and challenged with DNFB (C+) or vehicle (C–). Skin suspensions were evaluated for the expression of hCD2/Foxp3 and CD25. (**F**) Skin DLNs cells of sensitized B6 mice were stimulated in the absence or presence of Kaede-red total hCD2^{+} Tregs (25$^{hi/int}$), CD25^{hi} Tregs (25^{hi}), or CD25^{int} Tregs (25^{int}). (**G**) mRNAs for *Il10* (IL-10), *Tgfb1* (TGF-β), and *Ctla4* (CTLA-4) of Kaede-green CD25^{int} or CD25^{hi} Tregs, Kaede-red CD25^{int} or CD25^{hi} Tregs, or Kaede-green CD25^{int} Tregs in DLNs (D) or non-DLNs (N) were evaluated. The expression level in Kaede-green CD25^{int} Tregs was normalized to 1. Data are presented as means ± SD (n = 3) (**D**, **F**, and **G**). *$P < 0.05$ between indicated groups. (**F** and **G**). Numbers within plots or histograms indicate percentage of cells (**A**, **B**, and **E**).

Kaede-green Tregs of the DLNs or in non-DLNs (Figure 7A). Consistently, the frequency of the Kaede-red population in the CD25^{hi} population was greater than that in the CD25^{mid} population (Figure 7B). These CD25^{hi} Tregs showed higher levels of CCR4, CCR5, CCR7, CD44, CD103, CD11a, and CD54 than CD25^{int} Tregs in the Kaede-red subset (Figure 7C). On the other hand, the expression levels of CCR5 and CD103 of the CD25^{hi} subset in the Kaede-green cells tended to be lower than that in the Kaede-red cells, and the expression of CCR7 in Kaede-green Tregs was similar between CD25^{int} and CD25^{hi} subsets (Figure 7C).

We then examined the kinetics of T cell migration from the skin. Kaede/Foxp3$^{hCD2/hCD52}$ mice were sensitized and challenged as in Figure 3A and photoconverted immediately, 1, 2, or 3 days after challenge. The DLN cells were collected 24 hours after each photoconversion, and the number of Kaede-red CD4^{+}, CD4^{+}hCD2^{+}, CD4^{+}hCD2^{+}CD25^{hi}, and CD4^{+}hCD2^{+}CD25^{mid} cells migrating for 24 hours after photoconversion was determined (Figure 7D). The peak response of cell migration from the skin occurred on day 2 (between 48 and 72 hours after challenge) when the frequency of Tregs among CD4^{+} T cells migrating from

the skin was high (Figure 7D). In addition, $CD4^+hCD2^+CD25^{hi}$ cells were detected only at this time point (Figure 7D) and showed a high frequency of Kaede-red positivity, especially on day 2 (Figure 7D), suggesting that this subset is replaced by the skin-derived cells more readily than other subsets.

Strong immunosuppressive activity of $CD25^{hi}$ Kaede-red migratory Tregs. To evaluate whether $CD25^{hi}$ Tregs are localized in the skin during immune responses, Kaede/$Foxp3^{hCD2/hCD52}$ mice were sensitized and challenged as in Figure 3A. We detected a significant number of $CD25^{hi}$ Tregs in the challenged local skin, but few in the nonchallenged skin 48 hours after the challenge (Figure 7E), suggesting that $CD4^+hCD2^+CD25^{hi}$ cells are induced in the skin and migrate into the DLNs.

To determine the role of skin-derived $CD25^{hi}$ Tregs, Treg subsets were isolated from the DLNs of mice pretreated as in Figure 3A and cocultured with DLN cells from DNFB-sensitized mice. The $CD25^{hi}$ Tregs showed much stronger suppressive activity on T cell proliferation than the $CD25^{int}$ subset (Figure 7F).

We further examined the mRNA expression profiles of cytokines in the $CD25^{hi}$ Treg subsets. In agreement with the above in vitro result, Kaede-red $CD25^{hi}$ Tregs contained significantly higher amounts of *Il10*, *Tgfb1*, and *Ctla4* than Kaede-red $CD25^{int}$ Tregs in the DLNs, Kaede-green $CD25^{hi}$ or $CD25^{int}$ Tregs in the DLNs, or Kaede-green $CD25^{int}$ Tregs in the non-DLNs, except in the case of *Tgfb1* expression level between Kaede-red $CD25^{hi}$ Tregs and Kaede-green $CD25^{hi}$ Tregs in DLNs (Figure 7G). These results suggest that $CD25^{hi}$ Tregs migrating from the skin play a major suppressive role in cutaneous immune response.

Discussion

In this study, we found that memory/effector phenotype $Foxp3^+$ Tregs as well as $Foxp3^-$ non-Tregs migrated from the skin to DLNs in the steady state. The number of $CD4^+$ T cells in the skin and their migration to DLNs were prominently increased during a cutaneous immune response. Among the migrating T cells, $Foxp3^+$ Tregs constituted one of the major populations. Notably, the Tregs that migrated from the skin returned to the skin upon exposure to an antigen. The migrating Tregs held strong immunosuppressive effect and expressed high levels of mRNA for inhibitory mediators compared with LN-resident Tregs. Moreover, depletion of endogenous Tregs in vivo prolonged the CHS response. Finally, these circulating Tregs specifically included the $CD25^{hi}$ subset that showed an activated phenotype and a very strong inhibitory function on T cell proliferation, with high levels of mRNA for inhibitory mediators. These data suggest that Tregs circulate between blood, skin, and lymphoid tissues to regulate peripheral immune responses.

There have been a few studies that sought to address the possibility of T cell migration from the periphery to LNs. In their experiments, one report suggested that the memory/effector subset of $CD4^+$ T cells is the major constituent in the afferent lymph by cannulation of sheep (6, 11–13), and the other suggested the naive subset is dominant using subcutaneous injection of fluorescent-labeled lymphocytes (14). Recently, effector/memory phenotype of Tregs has been reported to migrate from blood to islet and to DLNs sequentially using an islet allograft model with transfer of in vitro–induced Tregs (30). However, since all the above experiments require traumatic or artificial procedures to label T cells in the periphery, it remains unknown whether endogenous T cells egress from the periphery into DLNs under pathophysiological conditions. In this study, using the Kaede-Tg system, we have clearly demonstrated that a subset of T cells with memory/effector phenotype migrates to DLNs in the steady state and during a cutaneous immune response. During the immune response, Tregs are the major constituents and they return to the skin upon exposure to an antigen. Therefore, as naive T cells circulate between blood and LNs, cells of the memory/effector T cell phenotype, especially Tregs, seem to circulate between blood and the skin. In this study, we used the skin as a representative of the peripheral tissues, but it would be of interest to explore this issue in other peripheral tissues, such as lungs and intestines.

To date, the roles of externally transferred Tregs in CHS have been reported (31); however, the regulatory activity of endogenous Tregs has not been fully assessed. In this study, we found that depletion of Tregs during the elicitation phase prolonged the CHS response. In addition, CHS-induced migratory Tregs suppressed the proliferation of DNFB-sensitized LN cells in a ratio as low as 1:100 (Tregs to LN cells), but such an inhibitory effect was not observed in non–antigen-specific mitogen-induced T cell proliferation systems. Therefore, Tregs circulating between the skin and LNs may inhibit not only T cells, but also antigen-presenting cells, such as dendritic cells, or antigen-presenting cell–T cell interactions. Moreover, subcutaneous injection of migratory Tregs into the skin suppressed CHS more markedly than that of LN-resident Tregs. Similar findings were observed when these Tregs were transferred intravenously (data not shown), suggesting that Tregs migrating from the skin hold a high immunosuppressive potential.

The $CD25^{hi}$ subset that migrated from the skin seems to have an activated phenotype, indicated by the positivity of CD25 and CD103. It has been reported that transfer of preactivated $CD25^+CD103^+$ cells strongly suppressed T cell proliferation (32) and $CD25^+CD103^+$ cells are the main producer of IL-10 after TCR stimulation (29). The $CD25^{hi}$ subset in our finding expresses high levels of CD103 and IL-10 and strong suppressive capacity and phenotype, consistent with an activated effector/memory Treg subset (28, 33). It should be noted that we demonstrate that the $CD25^{hi}$ subset was localized in the skin and only transiently migrated from the skin after CHS elicitation. Thus, the role of skin in generation, education, and spatiotemporal regulation of this $CD25^{hi}$ subset during immune responses needs to be elucidated in the future, which may lead us to understand the role of peripheral tissues in regulation of immune responses.

Notably, Treg cell circulation was remarkably induced during cutaneous immune responses. Therefore, we have focused on the roles of Tregs instead of effector/memory T cells migrating from the skin. In fact, the administration of migratory Tregs strongly suppressed CHS response at the later phase after a challenge (Figure 5A), and in vivo depletion of Tregs prolonged the CHS response, particularly during the later phase (Figure 4B). These results suggest that these circulating Tregs might be involved in the termination of immune responses. However, immune responses and homeostasis are regulated and maintained by the balance between Tregs and effector/memory T cells, and it has been thought that CHS occurs by the dominance of effector/memory T cells over Tregs. Hence, it is intriguing that the elicitation of CHS induces Tregs despite their possible antagonistic role for the development of acquired immune response. In this sense, it will be of interest to explore more the roles of effector/memory T cells and Tregs migrating from the skin in regulating immune response. Clarification of these issues will lead not only to understanding of the novel mechanism of cutaneous immune responses but also to control of systemic immune responses through modulating cutaneous immunity.

Methods

Mice and photoconversion. Tg mice carrying Kaede cDNA under the CAG promoter were established previously (17). These mice with B6 genetic background expressed photoconvertible Kaede in all of their cell types. It should be noted that the use of violet light (436 nm) rather than harmful UVA (320–400 nm) or UVB (290–320 nm) allowed us to photoconvert Kaede in the cells with no detectable damage (17).

Because of the moiety of its wavelength, violet light exposure penetrates through the skin to subcutaneous tissue, but not further (data not shown). Although the exposure of Kaede to violet light permanently changes its structure and photoconverted Kaede has a very long biological half-life in lymphocytes, cell proliferation dilutes photoconverted Kaede with newly synthesized nonphotoconverted Kaede, and after several cell divisions, the detection of red fluorescence becomes difficult (17). Moreover, exposure of the cells to violet light for 10 minutes has no effect on T and B cell proliferation (17). To exclude the immunomodulatory effect of photoconversion in vivo, we used the CHS model. Photoconversion of the abdominal skin immediately after sensitization on the abdomen did not affect CHS response (data not shown). When mRNA levels of *Il1b* were examined 6 hours after photoconversion (436 nm) or low-dose (3 kJ/m^2) UVB exposure, a significant increase of mRNA levels of *Il1b* was observed by UVB but not by photoconversion (Supplemental Figure 8). Therefore, we assume that photoconversion of the skin does not provoke significant inflammation in the skin or inflammatory stimuli in keratinocytes.

B6 Foxp3$^{hCD2/hCD52}$ mice were generated by homologous recombination in a B6-derived ES cell line using a targeting construct in which cDNA encoding a human CD2 and human CD52 fusion protein along with an intraribosomal entry site was inserted into the 3′ untranslated region of the endogenous Foxp3 locus (18). All CD4$^+$Foxp3$^+$ cells expressed hCD2, but CD4$^+$ Foxp3$^-$ cells did not (data not shown), indicating that the expression of the human CD2 reporter faithfully reflects the intracellular expression of Foxp3 in Foxp3$^{hCD2/hCD52}$ mice. Foxp3$^{hCD2/hCD52}$ mice (18) were intercrossed with Kaede-Tg mice to generate Kaede/Foxp3$^{hCD2/hCD52}$ mice for further evaluation. These mice were bred in specific pathogen–free facilities at Kyoto University or RIKEN. All experimental procedures were approved by the Institutional Animal Care and Use Committee of Kyoto University Faculty of Medicine and RIKEN.

Antibodies and flow cytometry. Fluorochrome-conjugated or biotinylated anti-human CD2, anti-mouse CD4, CD11a, CD11c, CD25, CD44, CD45RB, CD62L, CD69, CD103, GITR, CCR4, CCR5, and CCR7 mAbs were obtained from BD Biosciences, eBioscience, or Biolegend. Data were acquired using the JSAN system (Bay bioscience) or FACSCanto II flow cytometry system (BD Biosciences) and analyzed with FlowJo (TreeStar).

Cell preparation from the skin and cell sorting. Briefly, the ears were removed and split into dorsal and ventral halves, and cartilage was removed. The skin of the ears was floated on 0.25% trypsin/EDTA for 30 minutes at 37°C. Then the epidermis was peeled from the dermis, and both epidermis and dermis were minced with forceps. The minced tissues were incubated for 1 hours in collagenase II (Worthington Biochemical) containing hyaluronidase and DNaseI (Sigma-Aldrich). The cell suspensions were filtered with 40 μm of cell strainer.

For cell sorting, Kaede-red Tregs or Kaede-green Tregs were purified from inguinal and axillary LNs of Kaede/Foxp3$^{hCD2/hCD52}$ mice. Briefly, the mice were sensitized and challenged with DNFB in the same way as the B6 mice for DNBS-induced cell proliferation. Two days after the challenge, cells of abdominal skin were photoconverted, and single-cell suspensions were prepared from inguinal and axillary LNs 24 hours after photoconversion. The cells of each population were sorted by the FACSAria II flow cytometry system (BD Bioscience).

Photoconversion, CHS model, in vivo Treg depletion, and cell proliferation assay. Photoconversion of the skin was performed as described previously (17). Briefly, mice were anesthetized, shaved, and exposed to violet light at 95 mW/cm^2 with a 436-nm bandpass filter using Spot UV curing equipment (SP500; USHIO).

For the CHS model, mice were immunized by application of 25 μl of 0.5% DNFB (Nacalai Tesque) in 4:1 (wt/vol) acetone/olive oil to their shaved abdomens on day 0 and challenged on the right ear on day 5 with 20 μl of 0.3% (wt/vol) DNFB (34). Ear thickness was measured before and after challenge, and ear-thickness change was calculated.

For Treg depletion in vivo, mice were injected with Campath-1G Ab through the tail vein (0.5 mg/body) 1 day before the CHS challenge (22). The injection was repeated every 4 days throughout the experiment. The same amount of vehicle or rat IgG (0.5 mg/body; Sigma-Aldrich) was used as a control.

For DNBS- or TNBS-dependent cell proliferation, mice were sensitized with 50 μl of 0.5% DNFB (wt/vol) or 50 μl of 5% TNCB (Tokyo Kasei) (wt/vol) in acetone/olive oil (4/1; vol/vol) on the dorsal skin, and 5 days later, single-cell suspensions were prepared from inguinal and axillary LNs. CD25-positive cells were depleted from the cells by Auto-MACS (Miltenyi Biotec) using PE-labeled anti-mouse CD25 antibody (eBioscience) and magnetic microbeads coated with anti-PE (Miltenyi Biotec). Less than 1% of Foxp3$^+$ cells were present in the remaining LN cells. 7×10^5 LN cells/well in a 96-well plate were cultured in RPMI 1640 containing 10% FBS with or without 50 μg/ml DNBS (Alfa Aesar) for 3 days. For TNBS stimulation, the LN cells were incubated in 2.5 mM TNBS (Tokyo Kasei) in PBS for 20 minutes at 37°C and subsequently washed 3 times in PBS, and 7×10^5 cells/well in a 96-well plate were cultured in RPMI 1640 containing 10% FBS for 3 days. Cells were pulsed with 0.5 μCi ^{3}H-thymidine for the last 24 hours of culture and subjected to liquid scintillation counting.

For the proliferation assay of anti-CD3 stimulation, spleen CD4$^+$ cells deprived of CD25$^+$ cells were sorted by auto-MACS. Then, 5×10^4 cells/well were cultured in a 96-well plate coated with 1 μg/ml of anti-CD3 antibody for 72 hours. For the last 24 hours, cells were pulsed with 0.5 μCi ^{3}H-thymidine, and its incorporation was measured.

Quantitative RT-PCR analysis. Total RNA from purified cells was isolated with the RNeasy Mini Kit (QIAGEN). Quantitative RT-PCR with the Light Cycler real-time PCR apparatus was performed according to the instructions of the manufacturer (Roche) by monitoring the synthesis of double-stranded DNA during the various PCR cycles using SYBR Green I (Roche). For each sample, duplicate test reactions were analyzed for expression of the gene of interest, and results were normalized to those of the *Gapdh* mRNA.

In vivo immunosuppression assay. A total of 4×10^3 cells of isolated Kaede-red Tregs or Kaede-green Tregs in 20 μl PBS were subcutaneously injected into the ventral surface of each ear. Ear thickness was measured for each mouse before and at the indicated time point after elicitation with a micrometer, and the difference was expressed as ear swelling (n = 4–6 in each group).

Chemotaxis assay. Skin cell suspensions of Foxp3$^{hCD2/hCD52}$ mice were tested for transmigration across uncoated 5-μm transwell filters (Corning Costar Corp.) for 3 hours to CCL21 (R&D Systems) or medium in the lower chamber, and the numbers of cells that migrated to the lower chamber were determined by flow cytometry (35). The migration index was shown as a percentage of input by dividing with total input cells in upper chamber.

Statistics. Data were analyzed with the unpaired Student's 2-tailed t test unless otherwise stated. A P value of less than 0.05 was considered to be significant.

Acknowledgments

This study was supported in part by grants from the Ministry of Education, Culture, Sports, Science, and Technology of Japan and the Ministry of Health, Labor, and Welfare of Japan.

Received for publication August 24, 2009, and accepted in revised form December 16, 2009.

Address correspondence to: Kenji Kabashima, Department of Dermatology and Center for Innovation in Immunoregulative Technology and Therapeutics, Kyoto University, Yoshida-Konoe, Kyoto, 606-8501, Japan. Phone: 81.75.753.9502; Fax: 81.75.753.9500; E-mail: kaba@kuhp.kyoto-u.ac.jp. Or to: Michio Tomura, Laboratory for Autoimmune Regulation, Research Center for Allergy and Immunology, RIKEN, 1-7-22 Suehiro-cho, Tsurumi, Yokohama City, Kanagawa 230-0045, Japan. Phone: 81.45.503.9699; Fax: 81.45.503.9697; E-mail: tomura@rcai.riken.jp.

1. Korn T, Bettelli E, Oukka M, Kuchroo VK. IL-17 and Th17 cells. *Annu Rev Immunol.* 2009;27:485–517.
2. Sakaguchi S, Yamaguchi T, Nomura T, Ono M. Regulatory T cells and immune tolerance. *Cell.* 2008;133(5):775–787.
3. Lu LF, Rudensky A. Molecular orchestration of differentiation and function of regulatory T cells. *Genes Dev.* 2009;23(11):1270–1282.
4. Gowans JL, Knight EJ. The route of re-circulation of lymphocytes in the rat. *Proc R Soc Lond B Biol Sci.* 1964;159:257–282.
5. Gowans JL. The recirculation of lymphocytes from blood to lymph in the rat. *J Physiol.* 1959; 146(1):54–69.
6. Mackay CR, Marston WL, Dudler L. Naive and memory T cells show distinct pathways of lymphocyte recirculation. *J Exp Med.* 1990;171(3):801–817.
7. Matloubian M, et al. Lymphocyte egress from thymus and peripheral lymphoid organs is dependent on S1P receptor 1. *Nature.* 2004;427(6972):355–360.
8. Campbell DJ, Debes GF, Johnston B, Wilson E, Butcher EC. Targeting T cell responses by selective chemokine receptor expression. *Semin Immunol.* 2003;15(5):277–286.
9. Campbell JJ, et al. The chemokine receptor CCR4 in vascular recognition by cutaneous but not intestinal memory T cells. *Nature.* 1999;400(6746):776–780.
10. Homey B, et al. CCL27-CCR10 interactions regulate T cell-mediated skin inflammation. *Nat Med.* 2002;8(2):157–165.
11. Olszewski WL, Grzelak I, Ziolkowska A, Engeset A. Immune cell traffic from blood through the normal human skin to lymphatics. *Clin Dermatol.* 1995;13(5):473–483.
12. Olszewski WL. The lymphatic system in body homeostasis: physiological conditions. *Lymphat Res Biol.* 2003;1(1):11–21; discussion 21–24.
13. Mackay CR, Kimpton WG, Brandon MR, Cahill RN. Lymphocyte subsets show marked differences in their distribution between blood and the afferent and efferent lymph of peripheral lymph nodes. *J Exp Med.* 1988;167(6):1755–1765.
14. Debes GF, et al. Chemokine receptor CCR7 required for T lymphocyte exit from peripheral tissues. *Nat Immunol.* 2005;6(9):889–894.
15. Ando R, Hama H, Yamamoto-Hino M, Mizuno H, Miyawaki A. An optical marker based on the UV-induced green-to-red photoconversion of a fluorescent protein. *Proc Natl Acad Sci U S A.* 2002;99(20):12651–12656.
16. Mizuno H, et al. Photo-induced peptide cleavage in the green-to-red conversion of a fluorescent protein. *Mol Cell.* 2003;12(4):1051–1058.
17. Tomura M, et al. Monitoring cellular movement in vivo with photoconvertible fluorescence protein "Kaede" transgenic mice. *Proc Natl Acad Sci U S A.* 2008;105(31):10871–10876.
18. Komatsu N, et al. Heterogeneity of natural Foxp3+ T cells: a committed regulatory T-cell lineage and an uncommitted minor population retaining plasticity. *Proc Natl Acad Sci U S A.* 2009;106(6):1903–1908.
19. Fontenot JD, Rasmussen JP, Gavin MA, Rudensky AY. A function for interleukin 2 in Foxp3-expressing regulatory T cells. *Nat Immunol.* 2005; 6(11):1142–1151.
20. Randolph GJ, Ochando J, Partida-Sanchez S. Migration of dendritic cell subsets and their precursors. *Annu Rev Immunol.* 2008;26:293–316.
21. Hirahara K, et al. The majority of human peripheral blood CD4+CD25highFoxp3+ regulatory T cells bear functional skin-homing receptors. *J Immunol.* 2006;177(7):4488–4494.
22. Hale G, Cobbold SP, Waldmann H, Easter G, Matejtschuk P, Coombs RR. Isolation of low-frequency class-switch variants from rat hybrid myelomas. *J Immunol Methods.* 1987;103(1):59–67.
23. Wing K, Onishi Y, et al. CTLA-4 control over Foxp3+ regulatory T cell function. *Science.* 2008;322(5899):271–275.
24. Reiss Y, Proudfoot AE, Power CA, Campbell JJ, Butcher EC. CC chemokine receptor (CCR)4 and the CCR10 ligand cutaneous T cell-attracting chemokine (CTACK) in lymphocyte trafficking to inflamed skin. *J Exp Med.* 2001;194(10):1541–1547.
25. Randolph GJ, Ochando J, Partida SNS. Migration of dendritic cell subsets and their precursors. *Annu Rev Immunol.* 2007;26:293–316.
26. Yurchenko E, et al. CCR5-dependent homing of naturally occurring CD4+ regulatory T cells to sites of Leishmania major infection favors pathogen persistence. *J Exp Med.* 2006;203(11):2451–2460.
27. Baekkevold ES, et al. A role for CCR4 in development of mature circulating cutaneous T helper memory cell populations. *J Exp Med.* 2005;201(7):1045–1051.
28. Huehn J, et al. Developmental stage, phenotype, and migration distinguish naive- and effector/memory-like CD4+ regulatory T cells. *J Exp Med.* 2004;199(3):303–313.
29. Banz A, et al. A unique subpopulation of CD4+ regulatory T cells controls wasting disease, IL-10 secretion and T cell homeostasis. *Eur J Immunol.* 2003;33(9):2419–2428.
30. Zhang N, et al. Regulatory T cells sequentially migrate from inflamed tissues to draining lymph nodes to suppress the alloimmune response. *Immunity.* 2009;30(3):458–469.
31. Ring S, Oliver SJ, Cronstein BN, Enk AH, Mahnke K. CD4+CD25+ regulatory T cells suppress contact hypersensitivity reactions through a CD39, adenosine-dependent mechanism. *J Allergy Clin Immunol.* 2009;123(6):1287–1296 e1282.
32. Siegmund K, et al. Migration matters: regulatory T-cell compartmentalization determines suppressive activity in vivo. *Blood.* 2005;106(9):3097–3104.
33. Miyara M, et al. Functional delineation and differentiation dynamics of human CD4+ T cells expressing the FoxP3 transcription factor. *Immunity.* 2009;30(6):899–911.
34. Kabashima K, Arima Y, Miyachi Y. Contact dermatitis from lacquer in a 'Go' player. *Contact Dermatitis.* 2003;49(6):306–307.
35. Kabashima K, et al. Thromboxane A2 modulates interaction of dendritic cells and T cells and regulates acquired immunity. *Nat Immunol.* 2003;4(7):694–701.

Allergic contact dermatitis caused by a skin-lightening agent, 5,5′-dipropylbiphenyl-2,2′-diol

Kayoko Suzuki[1], Akiko Yagami[2] and Kayoko Matsunaga[2]

[1]*Department of Dermatology, Kariya Toyota General Hospital, 5-15, Sumiyoshi-cho, Kariya 448-8505, Japan and* [2]*Department of Dermatology, Fujita Health University School of Medicine, 1-98, Dengakugakubo, Kutsukake-cho, Toyoake 470-1192, Japan*

doi:10.1111/j.1600-0536.2011.01986.x

Key words: allergic contact dermatitis; cosmetics; 5,5′-dipropylbiphenyl-2,2′-diol; skin-lightening agent.

Many skin-lightening agents are currently available, including kojic acid, arbutin, hydroquinone, and 5,5′-dipropylbiphenyl-2,2′-diol (Fig. 1); the last of these is a relatively new skin-lightening agent that has been used in Japanese cosmetics since 2006. 5,5′-Dipropylbiphenyl-2,2′-diol is a biphenyl derivative, and downregulates melanin synthesis by inhibiting tyrosinase maturation, leading to accelerated tyrosinase degradation (1). Here, we report a case of allergic contact dermatitis caused by 5,5′-dipropylbiphenyl-2,2′-diol.

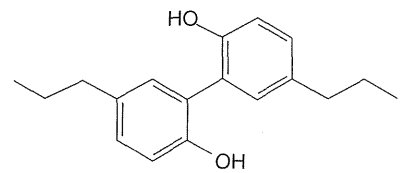

Molecular formula: $C_{18}H_{22}O_2$

Molecular weight: 270.372

CAS number: 20601-858-8

Fig. 1. Chemical formula of 5,5′-dipropylbiphenyl-2,2′-diol.

Case Report

A 45-year-old female presented with a 2-month history of an itchy erythematous rash on her cheek and neck. She had a negative history for dermatitis. Previously, she had been instructed to apply 0.3% prednisolone valerate acetate ointment twice daily by another dermatologist, but as cosmetic dermatitis was not suspected at the time, she had continued to use her cosmetics, with gradual worsening of the symptoms. We treated her with a regimen of oral prednisolone 20 mg daily for 4 days, olopatadine hydrochloride 10 mg daily for 1 week, and 0.1% hydrocortisone butyrate ointment, and advised her to stop using her cosmetics; her symptoms subsequently improved. Patch tests were performed with her personal cosmetics and 17 cosmetic allergens, using Finn Chambers® on Scanpor® tape. Readings were performed on D2 and D4 according to the International Contact Dermatitis Research Group guidelines. The patient showed positive reactions to a cream (+ on D2 and D4) and beauty essence (+ on D2 and D4), both of which were started 2 months prior to appearance of the rash. In the second patch test, with cosmetic ingredients provided by the cosmetic supplier, she reacted only to 5,5′-dipropylbiphenyl-2,2′-diol (0.5% pet., + on D2 and D4), which was present in both the cream and the beauty essence as a skin-lightening agent. The skin did not lighten over the area of the patch test with this chemical. Other cosmetic ingredients and cosmetic allergens gave negative reactions. Patch tests with 5,5′-dipropylbiphenyl-2,2′-diol 0.5% pet. in 4 control subjects gave negative results.

Discussion

Cosmetics with skin-lightening agents are popular in Japan. Cosmetics containing skin-lightening agents such as arbutin (2), hydroquinone and kojic acid have been reported to cause allergic contact dermatitis. 5,5′-Dipropylbiphenyl-2,2′-diol, an inhibitor of melanin synthesis synthesized by an oxidative coupling method (3), is a relatively new skin-lightening agent that has been marketed in Japan since 2006. Initial studies on this agent did not find adverse skin reactions. A double-blind test

Correspondence: Kayoko Suzuki, Department of Dermatology, Kariya Toyota General Hospital, 5-15 Sumiyoshi-cho, Kariya 448-8505, Japan. Tel: +81-566-21-2450; Fax: +81-566-22-2493. E-mail: kayokos@fujita-hu.ac.jp

Conflicts of interest: The authors have declared no conflicts of interest.

was conducted on 43 subjects to determine the efficacy of formulations containing 0.5% 5,5′-dipropylbiphenyl-2,2′-diol for the treatment of ultraviolet (UV)-induced pigmentation, and showed a significant difference in pigmentation score from placebo, with no adverse skin reactions (4). The skin-lightening effects of 6 months of application of 0.5% 5,5′-dipropylbiphenyl-2,2′-diol for facial hyperpigmentation were studied in 51 Japanese females, and no adverse effects were recorded (5). Another study investigating its effect on UV-induced facial skin hyperpigmentation in 300 Japanese females did not report adverse effects after application for 1 month (6).

The first case of allergic contact dermatitis caused by 5,5′-dipropylbiphenyl-2,2′-diol was described in 2009 (7). This first case reacted positively to 5,5′-dipropylbiphenyl-2,2′-diol 1% pet. In the present case, patch testing was performed with 5,5′-dipropylbiphenyl-2,2′-diol 0.5% pet., as the amount of 5,5′-dipropylbiphenyl-2,2′-diol permitted for use in cosmetics is less than 0.5%.

This case highlights the possibility of allergic contact dermatitis caused by skin-lightening agents in cosmetics. Determination of the optimum patch test concentration of 5,5′-dipropylbiphenyl-2,2′-diol may be required in further cases of allergic contact sensitivity caused by this agent.

References

1 Nakamura K, Yoshida M, Uchiwa H, Kawa Y, Mizoguchi M. Down-regulation of melanin synthesis by a biphenyl derivative and its mechanism. *Pigment Cell Res* 2003: **16**: 494–500.

2 Sugawara K, Kobayashi H, Teramae K, Ishii M, Kato A. A case of contact dermatitis due to arbutin. *Environ Dermatol* 2002: **9**: 146–148 (in Japanese).

3 Sartori G, Maggi R, Bigi F, Arienti A, Casnati G. Oxidative coupling of dichloroaluminium phenolates: highly selective synthesis of hydroxylated bi- and tetraaryls. *Tetrahedron* 1992: **48**: 9483–9494.

4 Takeda K, Yokota T, Ikemoto T, Kakishima H, Matsuo T. Inhibitory effect of a formulation containing 0.5% magnolignan (5,5′-dipropylbiphenyl-2,2′-diol) on UV-induced skin pigmentation. *Nishinihon J Dermatol* 2006: **68**: 288–292 (in Japanese).

5 Takeda K, Arase S, Sagawa Y et al. Clinical evaluation of the topical application of magnolignan (5,5′-dipropyl-biphenyl-2,2′-diol) for hyperpigmentation on the face. *Nishinihon J Dermatol* 2006: **68**: 293–298 (in Japanese).

6 Yokota T, Sasaki M. Development of whitening cosmetics with Magnolignan on inhibitory effect of the maturation of tyrosinase. *Fragr J* 2006: **34**: 80–83 (in Japanese).

7 Tsuruta K, Inaba Y, Nakagawa M, Matsunaga K. Allergic contact dermatitis from 5,5′-dipropylbiphenyl-2,2′-diol. *J Environ Dermatol Cutan Allergol* 2009: **3**: 368 (oral presentation abstract, in Japanese).

